Supporting Information

Zhang et al. 10.1073/pnas.1717116115

SI Materials and Methods

Protein Expression and Purification. The eTud domains of *Drosophila* Papi (residues 259–479), mTDRKH (residues 300–572), and BmPapi (residues 231–451) were cloned into a pET28-SMT3a vector containing an N-terminal Ulp1-cleavable His-SUMO tag. A fragment of Papi-eTud for GST pull-down assays was cloned into the pGEX-6p-1 vector. Wild-type Piwi-N (amino acids 1–94) and mutants were generated by cloning into the pRSFduet vector for expression in *E. coli*. A C-terminal Strep tag was introduced to Piwi-N by PCR. Flag-tagged wild-type Papi and mutants for co-IP assays were cloned into the pUAST-Flag vector. Myc-tagged Piwi and truncations were cloned in the pUAST-Myc vector. Full-length Piwi and Piwi-N (amino acids 1–94) with a C-terminal Strep tag were cloned into the pFast-HTb vector for expression using the Bac-to-Bac Baculovirus Expression System (Invitrogen) according to the manufacturer's protocol. All Papi mutants were generated using the Site-Directed Mutagenesis Kit (New England Biolabs) and verified by sequencing.

His-SUMO–tagged and GST-tagged recombinant proteins were expressed in *E. coli* BL21 (DE3) cells at 37 °C. All cells were grown to an OD_{600} of 0.8–1.0, and protein expression was induced with 0.2 mM isopropyl β-D-1-thiogalactopyranoside (IPTG) overnight at 16 °C. The cells were collected by centrifugation at 2,500 × *g* for 15 min and were lysed by French press (JNBIO) at 4 °C.

His-SUMO–tagged Papi-eTud was purified by affinity chromatography using a HisTrap column (GE Healthcare), and then the His-SUMO tag was removed by Ulp1 cleavage. The proteins were further purified by size-exclusive chromatography using a Superdex G75 HiLoad 16/60 column (GE Healthcare) in 10 mM Tris buffer (pH 8.0), 100 mM NaCl, and 1 mM DTT. The GST fusion proteins were purified by binding to glutathione-Sepharose beads (GE Healthcare) and were washed four times in pull-down buffer [100 mM NaCl, 20 mM Tris·HCl (pH 8.0)] to remove nonspecific binding.

Crystallization and Structural Determination. Purified Papi-eTud was concentrated to 15 mg/mL and crystallized by the vapor-diffusion method with the reservoir solution of 0.8 M succinic acid (pH 7.0). Purified Papi-eTud-D287A was concentrated to 15 mg/mL and crystallized by the vapor-diffusion method with the reservoir solution of 0.2 M malonate (pH 7.0) and 25% (wt/vol) PEG 3350. The crystals of Papi-eTud-D287A in complex with Piwi-R10me2s (amino acids 4–14) or Piwi-unme (amino acids 4–14) were obtained by mixing protein with peptide at 1:1.5 ratio and were grown in the same condition as the apo form. All crystals were grown at 17 °C and soaked in the reservoir solution supplemented with 15% glycerol before being flash-frozen in liquid nitrogen. Diffraction data were collected at beamline BL19U1 of the Shanghai Synchrotron Radiation Facility. The dataset was processed using the HKL-3000 program (1); statistics are shown in Table S1. The Papi-eTud apo structure was determined by molecular replacement using the eTud from human Tdrd2 (PDB ID code 5J39) as a search model. Papi–Piwi complex structures were solved by molecular replacement using the apo structure as a search model. All structural refinement was carried out using PHENIX (2). COOT was used for model building (3). All structural graphics were generated using the PyMOL Molecular Graphics System, version 1.8 (Schrödinger, LLC). Buried surface areas were calculated by PISA (4).

ITC Measurements. Piwi peptides used in ITC were synthesized (SciLight Biotechnology LLC). Wild-type or mutant Papi-eTud as well as Piwi peptides were dialyzed overnight in a buffer containing 10 mM Tris (pH 8.0) and 100 mM NaCl. ITC measurements were performed in duplicate at 20 °C using an iTC200 isothermal titration calorimeter (MicroCal, Inc.). The samples were centrifuged before the experiments to remove any precipitates. Experiments were carried out by 20 injections of 2 μL of 0.5 mM peptide solution into the sample cell containing 50 μM Papi-eTud, 10 mM Tris (pH 8.0), and 100 mM NaCl. Binding isotherms and SD were derived from nonlinear fitting using Origin Software version 7.0 (MicroCal, Inc.). The initial data point was routinely deleted. The ITC data were fit to a one-site binding model in 1:1 binding mode.

GST Pull-Down Assay. Purified wild-type and mutant GST-Papi-eTud fragments were immobilized on glutathione-Sepharose beads (GE Healthcare) for GST pull-down assays. Piwi-N proteins (amino acids 1–94) were added and incubated with GST-Papi-eTud or GST in a binding buffer [150 mM NaCl, 10 mM Tris (pH 8.0)] for 1 h with rotation at 4 °C. Then the bound protein was washed four times with the binding buffer and finally was eluted with the binding buffer supplied with 10 mM glutathione (reduced). The eluates were subjected to 15% SDS–PAGE followed by Coomassie blue staining.

Sample Preparation for MS. For pull-down of the Papi-eTud–associated proteins, we dissected roughly 300 ovaries from *w1118* flies. Ovaries were homogenized in 2 mL ice-cold extraction buffer [10 mM Hepes (pH 7.0), 100 mM KCl, 1.5 mM $MgCl_2$, 2 mM EDTA, 1.5 mM DTT, 1% Triton X-100, 10% glycerol, 0.5% Nonidet P-40, cOmplete Mini, EDTA-free protease inhibitor (Roche), and RNasin (Promega) or 300 μg/mL RNaseA] with 40 strokes. Lysates were centrifuged at 18,000 × *g* for 30 min at 4 °C. The supernatant was diluted with four volumes of NT2 buffer [25 mM Tris·HCl (pH 7.5), 150 mM NaCl, 1.5 mM $MgCl_2$, 1 mM DTT, 0.05% Nonidet P-40, cOmplete Mini EDTA-free protease inhibitor, and RNasin or 300 μg/mL RNaseA)] containing 40 μg GST-Papi-eTud or 20 μg GST protein as control (GST-Papi-eTud was added to GST at a molar ratio of 1:1). The incubation with GST-Papi-eTud or GST protein was performed for 12 h at 4 °C with rotation. Afterward, lysates were incubated with glutathione-Sepharose beads for 4 h at 4 °C with rotation. Beads were washed once with NT2 buffer containing 150 mM NaCl, once with NT2 buffer containing 300 mM NaCl, and twice with NT2 containing 150 mM NaCl without Nonidet P-40, each time for 10 min at 4 °C. The GST-Papi-eTud complex and GST control proteins were eluted twice with 50 μL of elution buffer [10 mM glutathione, 150 mM NaCl, 50 mM Tris (pH 8.0)] with agitation for 15 min each time at 4 °C. The eluate was stored at −80 °C until processing for MS analysis.

For analysis of the sDMA modification of Piwi-N, Sf9 cells were infected for 48 h at 28 °C, collected by centrifugation at 150 × *g* for 10 min, and resuspended in a buffer containing 20 mM Tris (pH 8.0), 500 mM NaCl, 25 mM imidazole, 5% (vol/vol) glycerol, 0.05% (vol/vol) Triton X-100, 1 mM PMSF, and cOmplete Mini EDTA-free protease inhibitor (Roche). His-Piwi-1–94-Strep protein was first purified by a HisTrap column (GE Healthcare) and eluted in a buffer containing 500 mM imidazole, 20 mM Tris (pH 8.0), and 500 mM NaCl. The eluate was then dialyzed against a buffer containing 100 mM Tris (pH 8.0), 150 mM NaCl, and 1 mM EDTA and was loaded on a StrepTrap HP column (GE Healthcare). Finally, the Strep-tagged proteins were eluted with the buffer containing 2.5 mM desthiobiotin, 100 mM Tris (pH 8.0), 150 mM NaCl, and 1 mM EDTA. For full-length Piwi

with an N-terminal His tag, the protein was purified with one HisTrap column (GE Healthcare).

Protein Precipitation and Digestion. Proteins were precipitated with trichloroacetic acid. The protein pellet was dried by SpeedVac (Thermo Scientific). The pellet was subsequently dissolved with 8 M urea in 100 mM Tris-Cl (pH 8.5). Tris(2-carboxyethyl)phosphine (TCEP) (final concentration, 5 mM) (Thermo Scientific) and iodoacetamide (final concentration, 10 mM) (Sigma) were added to the solution and incubated at room temperature for 20 and 15 min for reduction and alkylation, respectively. The solution was diluted four times and digested with trypsin at 1:50 (wt/wt) or AspN at 1:25 (wt/wt) (Promega).

LC/MS/MS Analysis of Peptide. The peptide mixture was loaded on a home-made 15-cm-long pulled-tip analytical column (75 μm i.d.) which was packed with 3-μm reverse-phase beads (Aqua C18; Phenomenex) connected to an Easy-nLC 1000 nanoflow HPLC system (Thermo Scientific) for MS analysis. The following 180-min HPLC gradient was used for peptide elution (buffer A: 0.1% formic acid in water; buffer B: 0.1% formic acid in acetonitrile): 0–5 min, 0–2% B; 5–140 min, 2–35% B; 140–160 min, 35–80% B; 160–170 min, 80% B; 170–171 min, 80–0% B, 171–180 min, 0% B. The flow rate was at 300 nL/min.

MS Conditions. Data-dependent MS/MS analysis was performed with a Q Exactive Orbitrap mass spectrometer (Thermo Scientific). Peptides eluted from the LC system were directly electrosprayed into the mass spectrometer with a distal 1.8-kV spray voltage. One acquisition cycle includes one full-scan MS spectrum (m/z 300–1,800) followed by the top 20 MS/MS events, sequentially generated on the first to the twentieth most intense ions selected from the full MS spectrum at a 27% normalized collision energy.

Data Analysis. The acquired MS/MS data were analyzed against a UniProt Knowledgebase (UniProtKB) drosophila database (released Nov. 11, 2016) using the Integrated Proteomics Pipeline (IP2, integratedproteomics.com/). To accurately estimate peptide probabilities and false-discovery rates, we used a decoy database containing the reversed sequences of all the proteins appended to the target database. Carbamidomethylation (+57.02146) of cysteine was considered as a static modification and arginine methylation as a variable modification. PEAKS 8.5 software was used for further peptide and protein quantification (www.bioinfor.com/peaks-studio/).

Co-IP. S2 cells were maintained in *Drosophila* Schneider's Medium (Invitrogen) supplemented with 10% heat-inactivated FBS, 100 units/mL penicillin, and 100 mg/mL streptomycin. The cells were incubated at 25 °C in a humidified air atmosphere. S2 cells were seeded at 1×10^6 cells/mL. Papi-FL, 64–210, 211–576, and 259–479 fragments were cloned into pUAST-Flag to generate Papi-Flag proteins. Piwi-FL, 1–94, and 95–843 were cloned into pUAST-Myc to generate Myc-Piwi proteins. Plasmid transfection was carried out using Cellfectin II Reagent (Invitrogen) according to the manufacturer's instructions. For all transfection experiments, a ubiquitin-Gal4 construct was cotransfected with the pUAST expression vectors. For immunoprecipitation, after 48 h of expression, cells were lysed in immunoprecipitation buffer [50 mM Tris·HCl (pH 8.0), 150 mM NaCl, 1% Nonidet P-40, 10% glycerol, 1.5 mM EDTA] supplied with cOmplete Mini EDTA-free protease inhibitor (Roche). Cell lysates were precleared by Protein A beads (Santa Cruz) and then were incubated with the indicated antibodies. The incubation with antibodies was performed for 12 h at 4 °C with rotation. Afterward, lysates were incubated with Protein A beads (Santa Cruz) for 4 h at 4 °C with rotation. Beads were washed four times with the immunoprecipitation buffer, 10 min each time, at 4 °C. Finally, SDS loading was added, and the samples were boiled at 95 °C for 5 min and substrated to SDS/PAGE electrophoresis analysis followed by Western blot. Western blot was done according to standard protocols. Briefly, protein samples were resolved by SDS/PAGE and transferred to 0.45-μm nitrocellulose membranes (GE Healthcare) before blotting overnight with primary antibodies in 0.075% Tween 20 in 1× TBS (TBST). After three washes with TBST, incubation with HRP-coupled secondary antibodies, and three more washes in TBST, the membranes were incubated with Pierce ECL Western Blotting Substrate (Thermo) and imaged using a ChemiDoc MP imaging system (Bio-Rad). The following antibodies were used in the immunoprecipitation or Western blot analyses: rabbit anti-Flag antibody (Proteintech) and rabbit anti-Myc antibody (Proteintech) for immunoprecipitation using dilutions of 1:400 for immunoprecipitations, and mouse anti-Flag (Sigma), mouse anti-Myc (Proteintech), and mouse anti-HRP (Proteintech) using dilutions of 1:5,000 for all antibodies.

For the Western blot of the GST-Papi-eTud pull-down assay from ovary lysate, the work flow was similar to the procedure used to prepare the MS sample, but glutathione-Sepharose beads (GE Healthcare) alone or GST protein was added as a negative control, and the ovary lysate was supplied with RNaseA (300 μg/mL). The pull-down samples were substrated to Western blot, and the following antibodies were used: rabbit anti-Piwi (against Piwi amino acids 350–450) (1:500; ab5207; Abcam), Ago3 (1:500; MaB Technologies), Aub (1:500; GeneTex), mouse anti–ATP-5A (1:1,000; 15H4C4; Abcam), rabbit anti–Piwi-R10-me2s (1:5,000; described below), and rabbit anti-GST (1:1,500; Proteintech).

Antibody Generation. Rabbit anti–Piwi-R10-me2s antibody was generated against DQGRGR-(symmetrical-2me)R-RPLNEC (Piwi amino acids 4–15) and CDQGRGR-(symmetrical-2me)RRPL (Piwi amino acids 4–15); in both cases, cysteine was added for antibody purification peptides. The peptides were immune to rabbits, and the antiserum was collected to flow first through the proA column, followed by flowing and eluting through the Piwi-R10me2s peptide-immobilized column and then successively through the Piwi-R10me2as peptide-immobilized column and Piwi-unme-immobilized peptide. Finally, the flow-through production was collected (PTM Biolabs, Inc.). Rabbit anti-Papi antibody was generated against Papi-eTud (amino acids 259–479) and was used to detect Papi expression in the ovary lysate of *w1118*, *papi*$^{-/-}$, or Papi-mutant rescue flies.

Dot Blot Assay. Different amounts of Piwi-R7me2s, Piwi-R9me2s, Piwi-R10me2s, Piwi-R11me2s, and Piwi-unme peptides were spotted on a nitrocellulose membrane (GE Healthcare). Then the membrane was blocked with 5% milk in TBST for 1 h at room temperature, followed by the incubation of Piwi-R10me2s antibody at room temperature for 1 h. After three rounds of washes with TBST, membranes were incubated with a 1:5,000 dilution of HRP-conjugated anti-rabbit IgG secondary antibody. Last, the membranes were incubated with Pierce ECL Western Blotting Substrate (Thermo) and imaged using a ChemiDoc MP imaging system (Bio-Rad).

Quantitative RT-PCR. RNA was isolated from about 20 drosophila ovaries of the indicated genotypes using TRIzol reagent (Invitrogen) following the manufacturer's protocol, and quantification of the transposon transcripts by quantitative RT-PCR was performed on QuantStudio 6 (ABI). Primers for test were described previously (5).

Fly Husbandry. Flies were grown at 25 °C. For ovary dissection, flies aged 2–6 d were given fresh food with yeast for 2 d and then were dissected after brief immobilization by CO_2 anesthesia. For fertility counts of *w1118*, *papi*$^{-/-}$, or Papi-mutant rescue flies, 15

2- to 4-d-old virgin females of the indicated genotypes were crossed with three 2-d-old w1118 males. In the following 10 d, the eggs laid in each vial were counted to test the fertility rate of the indicated genotypes.

Transgenic Flies. Papi-KO flies with a 317-bp deletion and frameshift mutations were generated by CRISPR/Cas9 using guide RNAs, sgRNA1 CGAGCCGCCTTAACCGCATCGGG, and sgRNA2 TGCTGTTGGTGGGAGATCTGCGG, as previously reported (6). For papi transgene rescue flies, full-length Papi wild-type, Y328, D348A, and Y348A/D348A double-mutant cDNA was cloned into the pUASp vector with the attB site separately and was injected into attp3#-68A4 (y[1] M{vas-int.Dm}ZH-2A w[*]; P{CaryP}attP2) embryos to generate transgenic flies. The expression of the transgene was driven by the Act5C-Gal4 (BS3954) driver and was crossed to *papi*$^{-/-}$ flies to perform the rescue experiments. Fly microinjection was conducted by the *Drosophila* Core Facility, Institute of Biochemistry and Cell Biology, Chinese Academy of Sciences. All fly strains used in the study are available via the Bloomington *Drosophila* Stock Center at Indiana University.

Data Analysis of Piwi-Bound piRNAs in Wild-Type and *papi*$^{-/-}$ Mutants. Piwi-bound RNA sequence data of wild-type and *papi*$^{-/-}$ ovaries were downloaded from the National Center for Biotechnology Information (NCBI) Gene Expression Omnibus (GEO) database (accession code GSE83698) and were analyzed as described in previous studies (7).

1. Otwinowski Z, Minor W (1997) Processing of X-ray diffraction data collected in oscillation mode. *Methods Enzymol* 276:307–326.
2. Adams PD, et al. (2010) PHENIX: A comprehensive Python-based system for macromolecular structure solution. *Acta Crystallogr D Biol Crystallogr* 66:213–221.
3. Emsley P, Cowtan K (2004) Coot: Model-building tools for molecular graphics. *Acta Crystallogr D Biol Crystallogr* 60:2126–2132.
4. Krissinel E, Henrick K (2007) Inference of macromolecular assemblies from crystalline state. *J Mol Biol* 372:774–797.
5. Liu L, Qi H, Wang J, Lin H (2011) PAPI, a novel TUDOR-domain protein, complexes with AGO3, ME31B and TRAL in the nuage to silence transposition. *Development* 138: 1863–1873.
6. Yu Z, et al. (2013) Highly efficient genome modifications mediated by CRISPR/Cas9 in Drosophila. *Genetics* 195:289–291.
7. Hayashi R, et al. (2016) Genetic and mechanistic diversity of piRNA 3′-end formation. *Nature* 539:588–592.

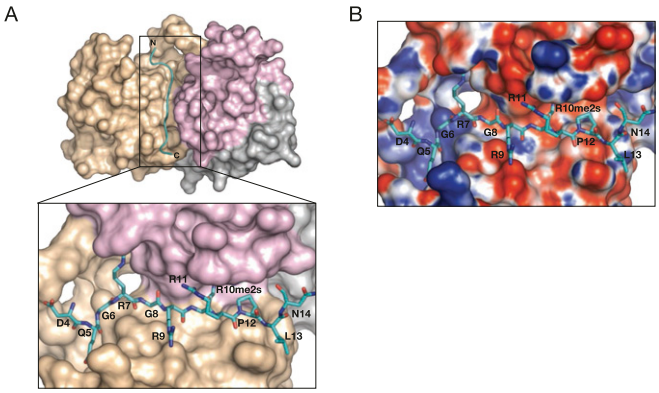

Fig. S1. Piwi peptide bound on the concave surface of Papi-eTud. (*A*) Piwi peptide bound on the concave surface of Papi-eTud formed by the Tudor core and the SN domain. Color codes: Tudor core, pink; SN domain, wheat; Piwi-R10me2s peptide, teal. (*B*) The positioning of the bound Piwi peptide (stick representation) within the Papi-eTud–binding site (electrostatic surface representation).

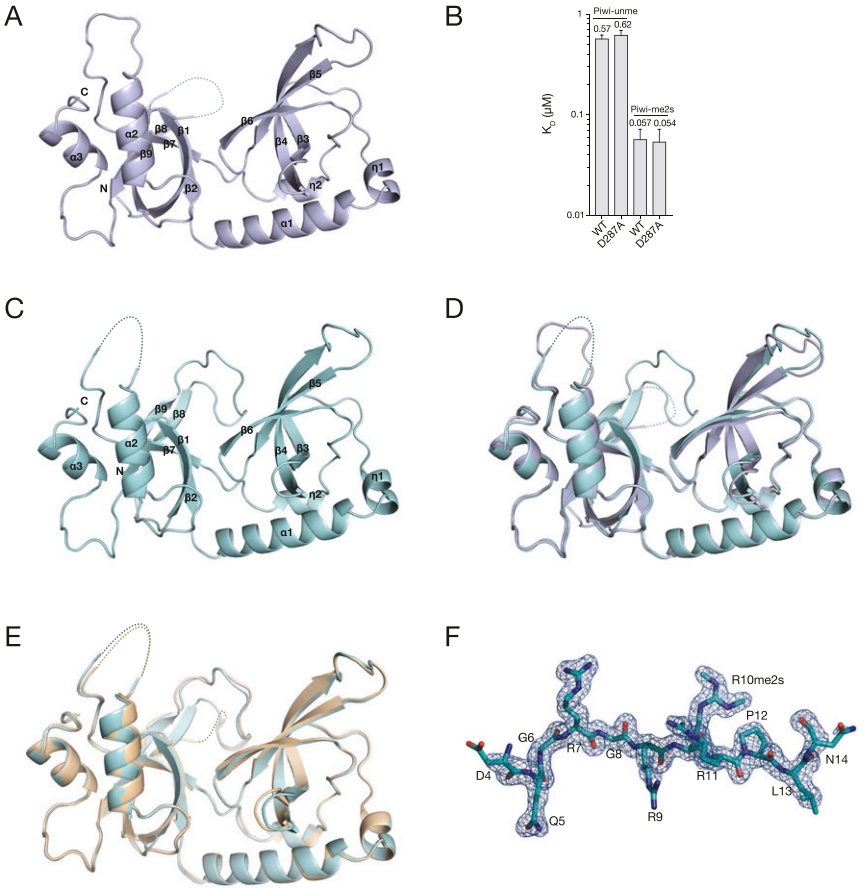

Fig. S2. Structure of the eTud domain of Papi in apo form. (*A*) The overall structure of Papi-eTud. (*B*) Comparison of the binding affinities of Piwi-unme and Piwi-R10me2s by wild-type Papi-eTud and the D287A mutant. (*C*) The overall structure of Papi-eTud-D287A. (*D*) Superimposition of the wild-type Papi-eTud and the D287A mutant. (*E*) Superimposition of the apo form and complex form of Papi-eTud. (*F*) The *2Fo-Fc* electron density map (contoured at 1.0 σ cutoff, blue mesh) for the Piwi peptide.

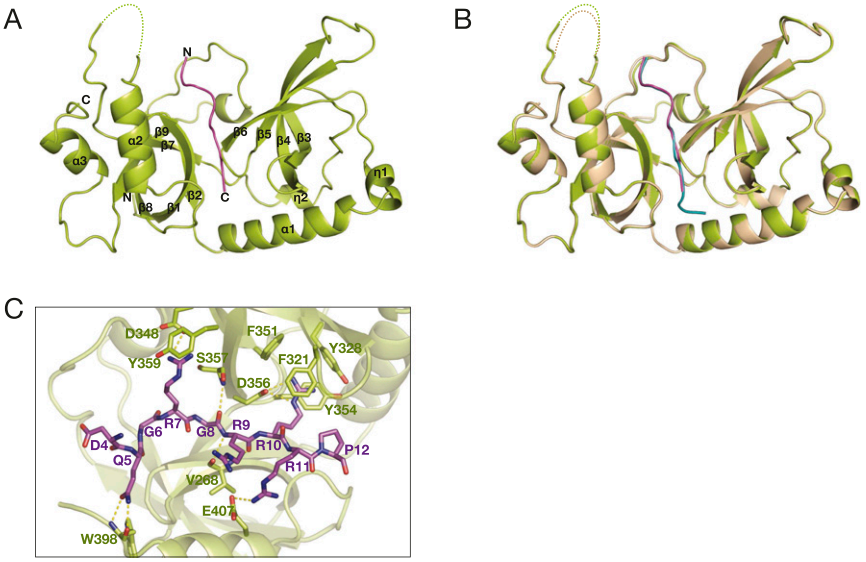

Fig. S3. Structure of Papi-eTud in complex with Piwi-unme. (*A*) The overall structure of the eTud domain of Papi in complex with the unmethylated Piwi peptide. Papi-eTud is shown in green. Piwi-unme is shown in magenta. (*B*) Superimposition of Papi–Piwi-R10me2s and Papi–Piwi-unme. (*C*) Detailed interactions of unmethylated Piwi recognized by Papi-eTud.

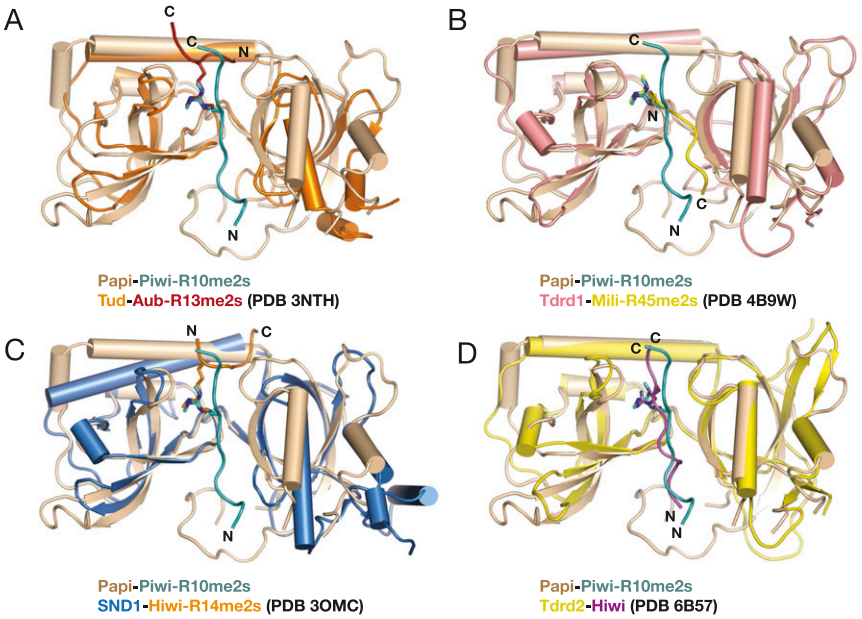

Fig. S4. Structural comparisons of the Papi-eTud–Piwi complex and other eTud–ligand complexes. Papi–Piwi-R10me2s is superimposed with previously reported structures of eTud domains of Tdrd proteins in complex with (G/A)R motif peptides of PIWI proteins. Papi-eTud is shown in wheat, and the Piwi peptide is shown in teal. The symmetrical dimethyl arginine is represented as a stick mode. (*A*) Superimposition of Papi–Piwi and the 11th eTud domain of Tud (orange) in complex with Aub-R13me2s (raspberry) (PDB ID code 3NTH). (*B*) Superimposition of Papi–Piwi and mouse Tdrd1 eTud domain (pink) in complex with Mili-R45me2s (yellow) (PDB ID code 4B9W). (*C*) Superimposition of Papi–Piwi and the eTud domain of SND1 (blue) in complex with Hiwi-R14me2s (orange) (PDB ID code 3OMC). (*D*) Superimposition of Papi–Piwi and the eTud domain of Tdrd2 (yellow) in complex with Hiwi-R10unme (purple) (PDB ID code 6B57).

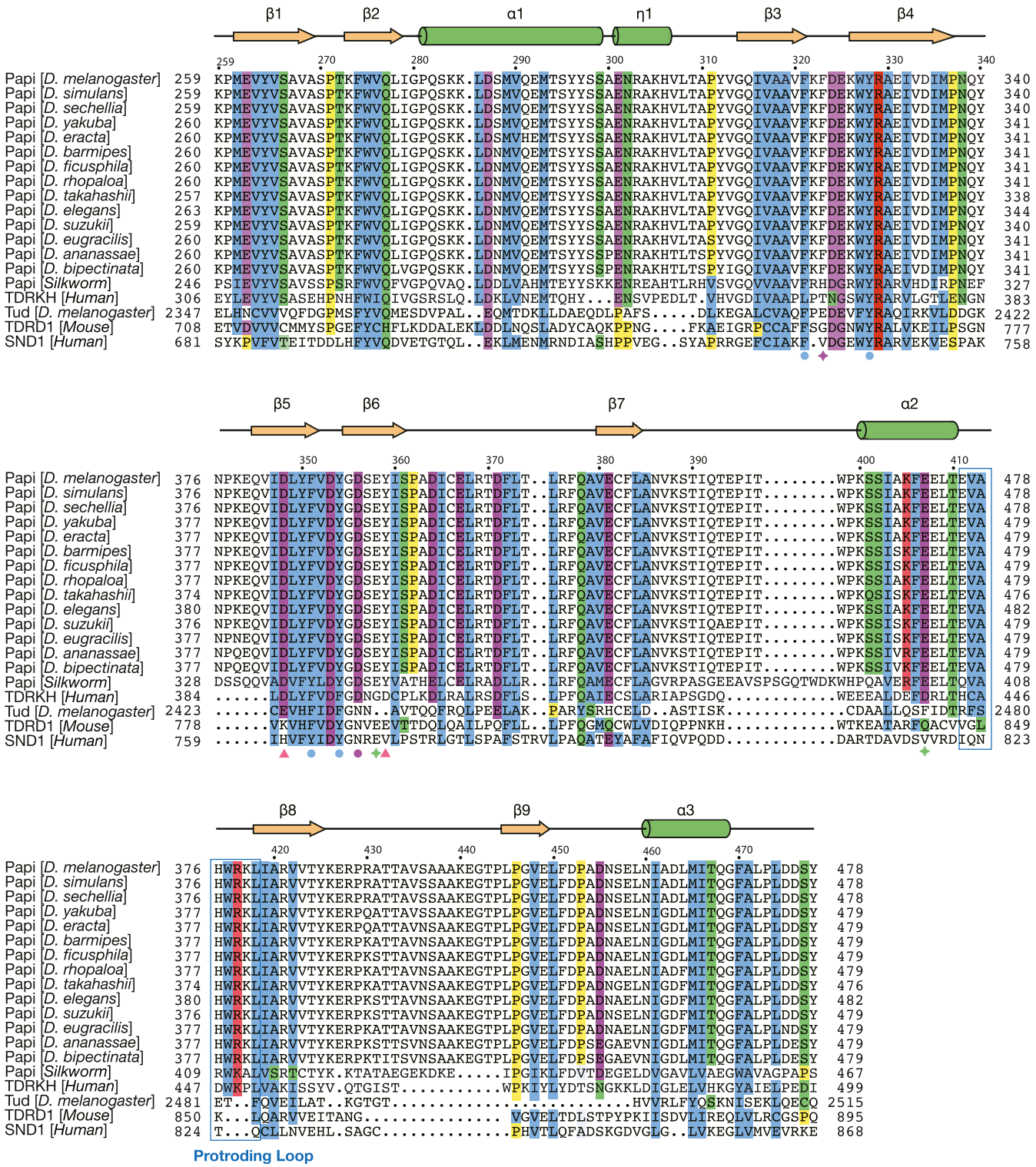

Fig. S5. Sequence alignment of eTud domains. Sequence alignment of *Drosophila* Papi extended Tudor domain and other proteins' extended Tudor domains. The cartoon of the secondary structure (yellow indicates β-strands; red indicates α-helices) is based on Papi-eTud (amino acids 259–479). Colors in the chart were generated by conservation in the Clustal X mode of Jalview software. In general, blue denotes the nonpolar amino acids, green denotes hydrophilic amino acids, purple denotes acidic amino acids, red indicates basic amino acids, and proline is labeled in yellow. Specifically, the residues forming the aromatic cage are indicated by blue dots at the bottom of the alignment, the residue interacting with R10 is indicated by a purple cross prism, residues interacting with R7 in the Piwi-R10me2s peptides are indicated by pink triangles, and residues interacting with R9 and R11 are indicated by green cross prisms.

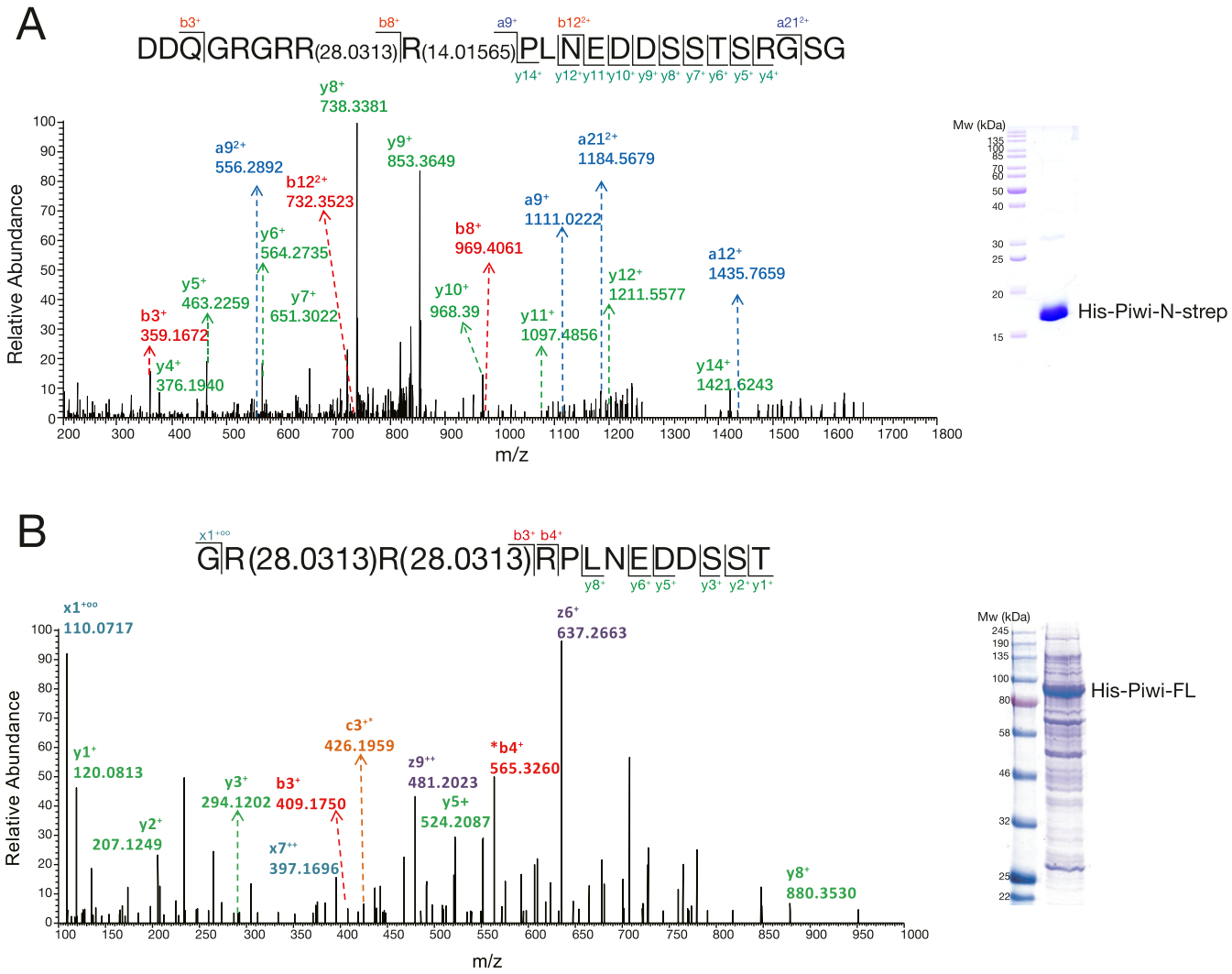

Fig. S6. MS/MS spectrum analysis of the arginine dimethylation modification on Piwi-N and full-length Piwi expressed in sf9 cells. (*A*) MS/MS spectrum of R10 di-methyl and R11 methyl peptide of the His-Piwi-1–94-strep protein: higher-energy collisional dissociation (HCD) MS/MS spectrum recorded on the [M+2H]+2 ion at *m/z* 1,280.61 of the modified Piwi peptide DDQGRGRR (28.0313)R(14.01565)PLNEDDSSTSRGSG harboring one R10 di-methyl and one R11 methyl site. Ions observed are labeled in the spectrum and indicate that R10 and R11 of the protein are modified with di-methylation and methylation, respectively. (*B*) MS/MS spectrum of a R9-dimethyl and R10-dimethyl peptide of His-Piwi-FL expressed in Sf9 cells: (HCD) MS/MS spectrum recorded on the [M+2H]2+ ion at *m/z* 780.89 of the modified Piwi peptide GR(28.0313)R(28.0313) RPLNEDDSST harboring two dimethyl-R sites. Ions observed are labeled in the spectrum and indicate that R9 and R10 of PIWI are both dimethylated. The asterisk and cycle symbols indicate the neutral loss of ammonia and water, respectively.

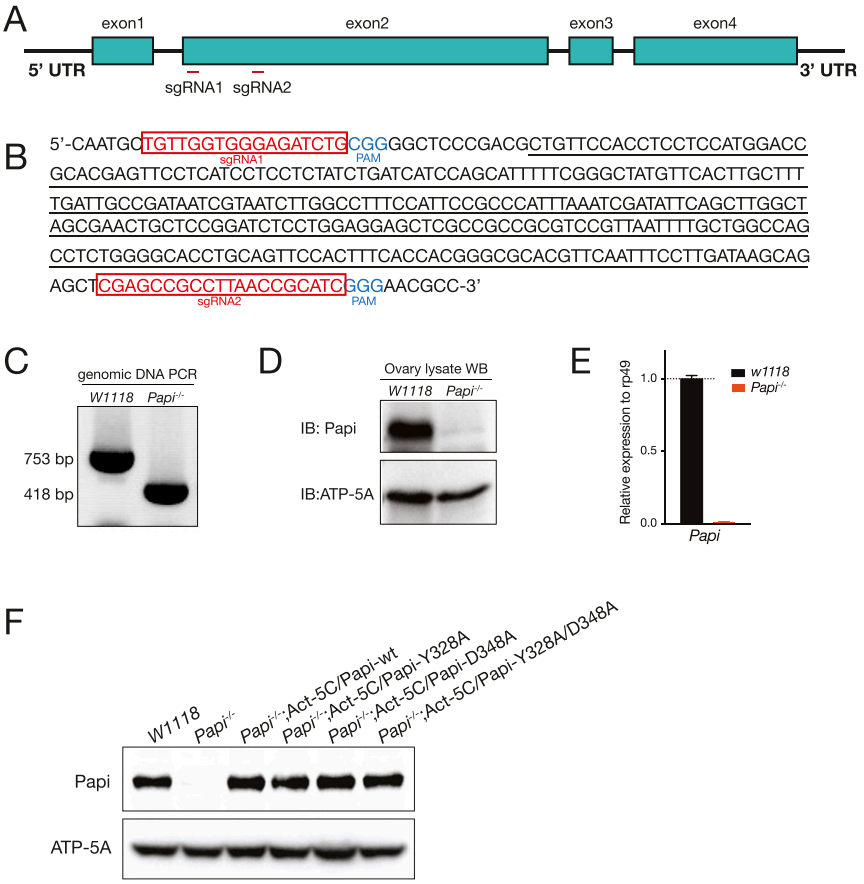

Fig. S7. Generation of *papi*$^{-/-}$ mutants. (*A*) The *papi* gene locus and guiding RNAs used to make *papi*$^{-/-}$ mutant files. SgRNA1 and sgRNA2 (red lines) were used to generate a Cas9-induced papi-null allele (*papi*$^{-/-}$ mutants). (*B*) Parts of the *papi* genomics sequence illustrating features of the CRISPR/Cas9-mediated *papi*-null allele. SgRNAs and protospacer-adjacent motifs (PAMs) are highlighted. Deleted nucleotides are underlined. Resulting *papi*$^{-/-}$ mutants were back-crossed to the control homogeneous background for five generations to ensure background clearance. (*C*) PCR analysis confirms that *papi*$^{-/-}$*-KO* is a deletion allele. DNAs were from whole files. Genotypes: *w1118*, control; *papi*$^{-/-}$, mutants. (*D*) Western blot (WB) confirms the loss of detectable Papi protein in *papi*$^{-/-}$ mutants' ovaries. (*E*) RT-PCR assay to test the Papi mRNA level in *w1118* and *papi*$^{-/-}$ mutants. (*F*) Western blot analysis of Papi protein expression in *w1118*, *papi*$^{-/-}$, and *papi*-mutant rescue flies. The genotypes of the flies are indicated.

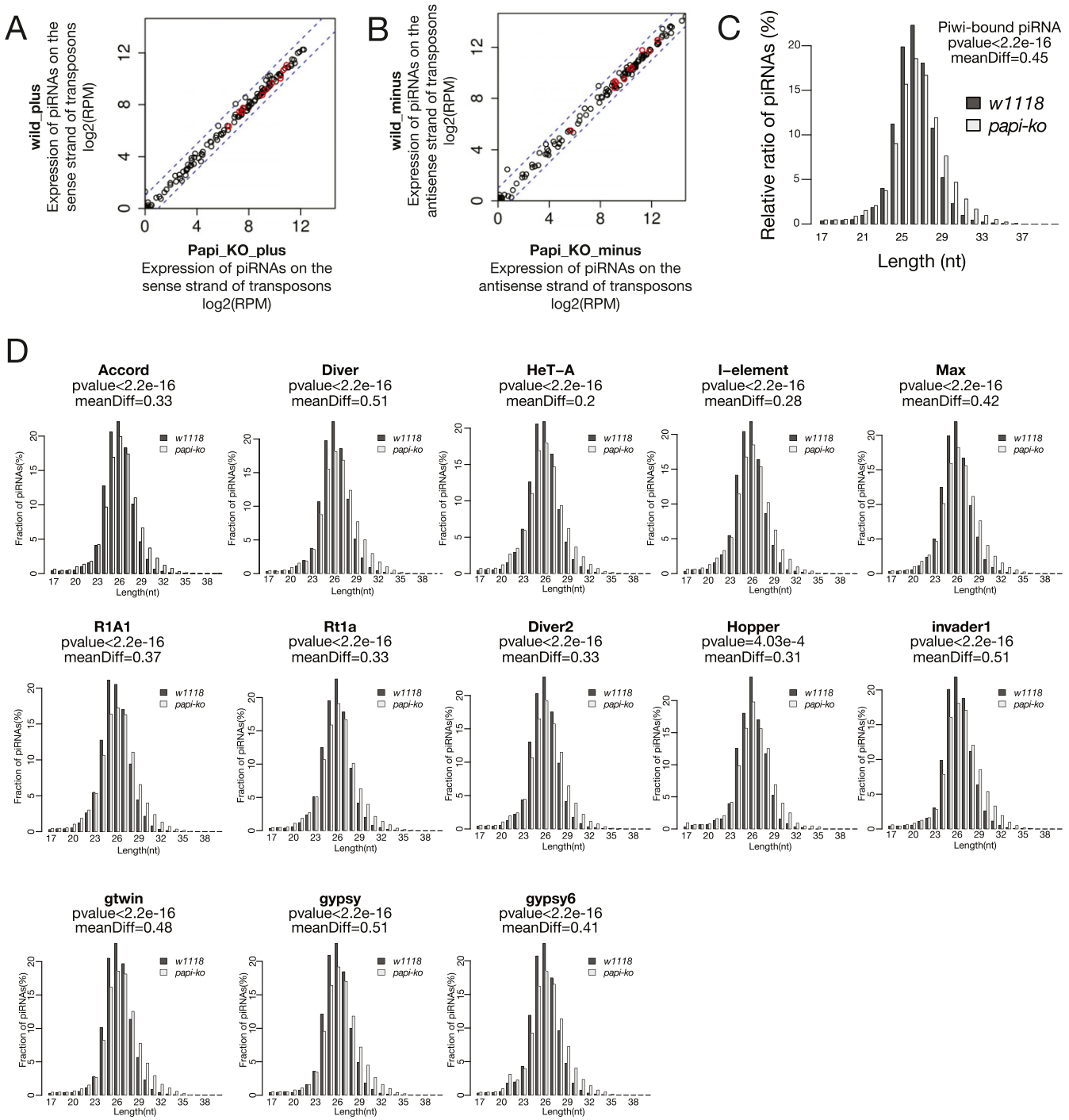

Fig. S8. Length of piRNAs derived from 13 transposons of interest increased, although the changes in TE expression in Piwi-bound piRNAs from wild-type and *papi*-KO flies' ovaries were not significant. (*A* and *B*) Expression correlation of Piwi-bound piRNAs derived from each transposon in wild-type and *papi*-KO flies' ovaries. Dots circled by red denote TE expression correlations of the 13 transposons of interest; the region between the two dashed lines denotes the TEs whose expression changes by twofold in *papi*-KO flies' ovaries versus wild-type ovaries. (*A*) Correlation of piRNA expression on the sense strand of transposons. (*B*) Correlation of piRNA expression on the antisense strand of transposons. (*C*) Distribution of the length of Piwi-bound piRNAs derived from each transposon in wild-type and *papi*-KO flies' ovaries. (*D*) Distribution of the length of piRNAs derived from 13 transposons of interest was increased. Note: Piwi-bound RNA sequence data from a previous study in *A*–*C* were downloaded from the NCBI GEO database (accession code GSE83698) and were analyzed according to the authors' descriptions; *P* values were calculated as a two-sided *t* test, and mean increasing lengths of piRNAs are listed above the charts (1).

1. Hayashi R, et al. (2016) Genetic and mechanistic diversity of piRNA 3′-end formation. *Nature* 539:588–592.

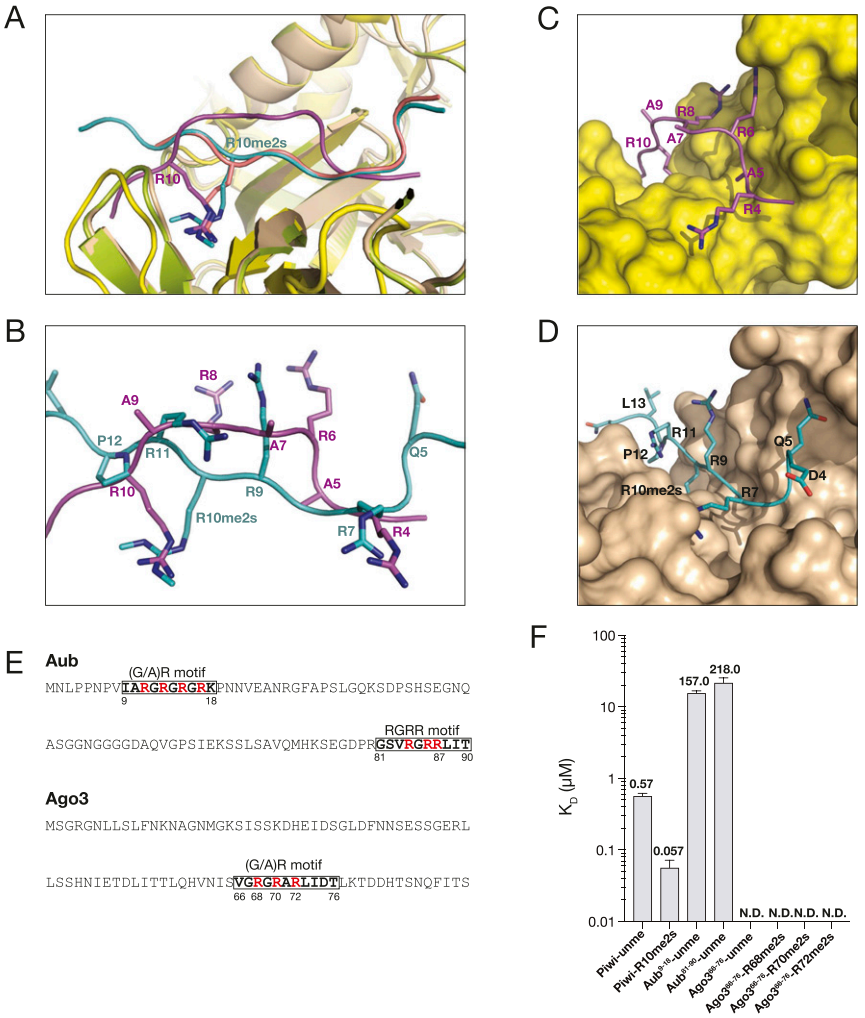

Fig. S9. Different binding mode in Papi and its homologs. (*A*) Superimposition of the structures of Papi-eTud (green) in complex with Piwi-unme (salmon), Papi-eTud (wheat) in complex with Piwi-R10me2s (teal), and Tdrd2-eTud (yellow) in complex with Hiwi (purple). Arginine residues that insert into the aromatic cage are indicated. (*B*) Superimposition of Piwi-R10me2s and Hiwi peptides. (*C*) The (G/A)R motif of Hiwi bound on the surface of Tdrd2-eTud. (*D*) The RGRRR motif of Piwi bound on the surface of Papi-eTud. (*E*) Sequences of the 90 N-terminal amino acids of Aub and Ago3. The (G/A)R motifs used in ITC experiments are boxed. Amino acid positions are indicated. Arginine residues are shown in red. (*F*) Bar graph representations of the binding affinities of Papi-eTud to Aub$^{9–18}$-unme, Aub$^{81–90}$-unme, Ago3$^{66–76}$-unme, Ago3$^{66–76}$-R68me2s, Ago3$^{66–76}$-R70me2s, and Ago3$^{66–76}$-R72me2s peptides monitored by ITC. N.D., not detected.

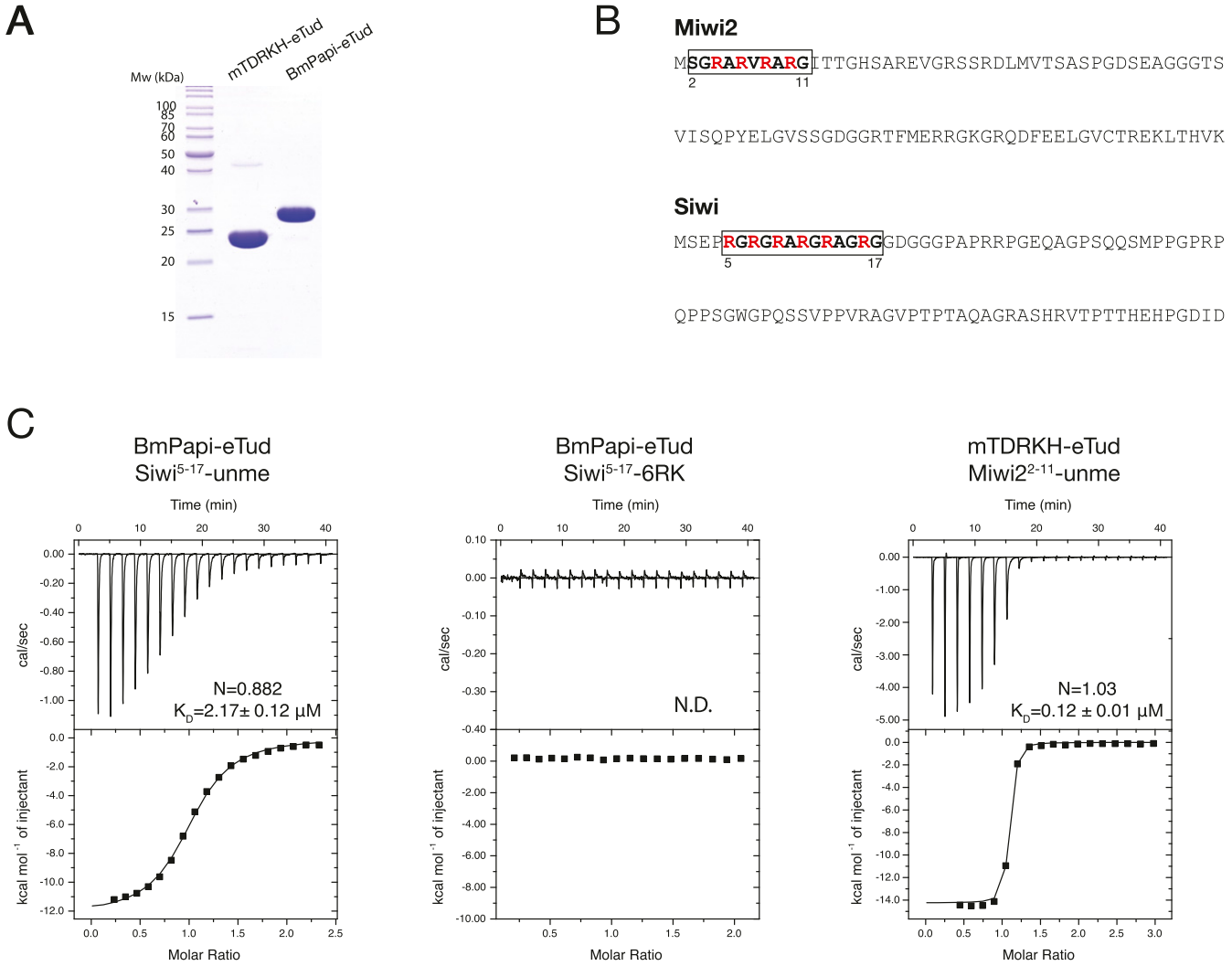

Fig. S10. Binding affinities of Papi homologs to Miwi2 and Siwi. (*A*) SDS/PAGE shows the purified mTDRKH-eTud (residues 300–527) and BmPapi-eTud (residues 231–451). (*B*) Sequences of the 90 N-terminal amino acids of Miwi2 and Siwi. The (G/A)R motifs used in ITC experiments are boxed. Amino acid positions are indicated. Arginine residues are shown in red. (*C*) Binding affinities of mTDRKH-eTud and BmPapi-eTud to Miwi2$^{2–11}$-unme and Siwi$^{5–17}$-unme peptides as monitored by ITC. Siwi$^{5–17}$-6RK indicates the six arginine residues shown in *B* are replaced by lysine. N.D., not detected.

A

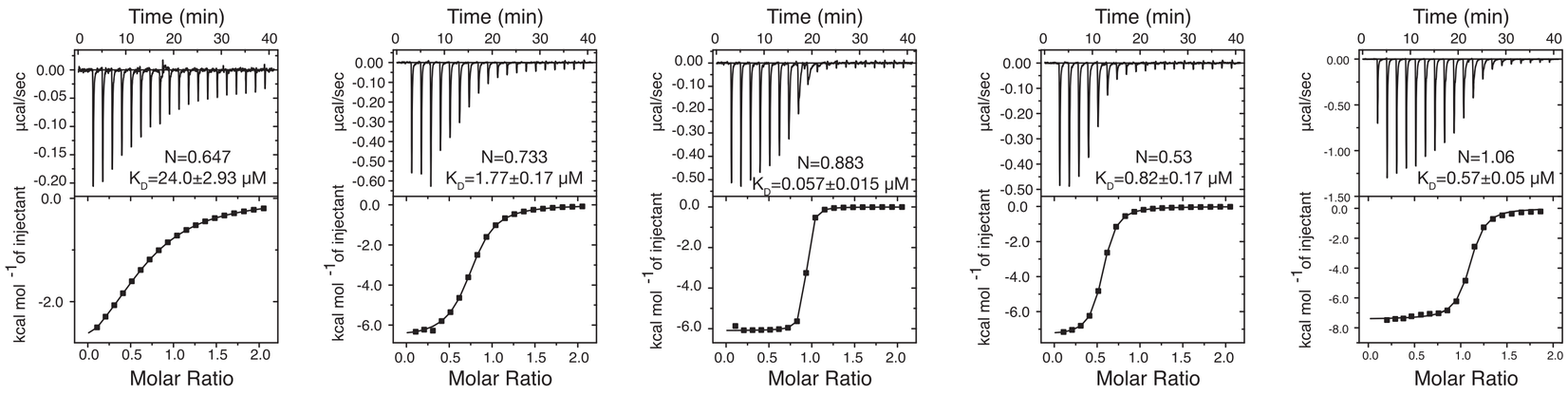

Papi-eTud with Piwi-R7me2s | **Papi-eTud with Piwi-R9me2s** | **Papi-eTud with Piwi-R10me2s** | **Papi-eTud with Piwi-R11me2s** | **Papi-eTud with Piwi-unme**

B

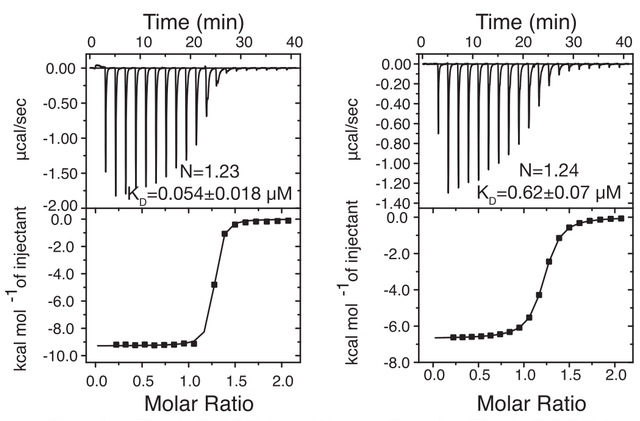

Papi-eTud-D287A with Piwi-R10me2s | **Papi-eTud-D287A with Piwi-unme**

C

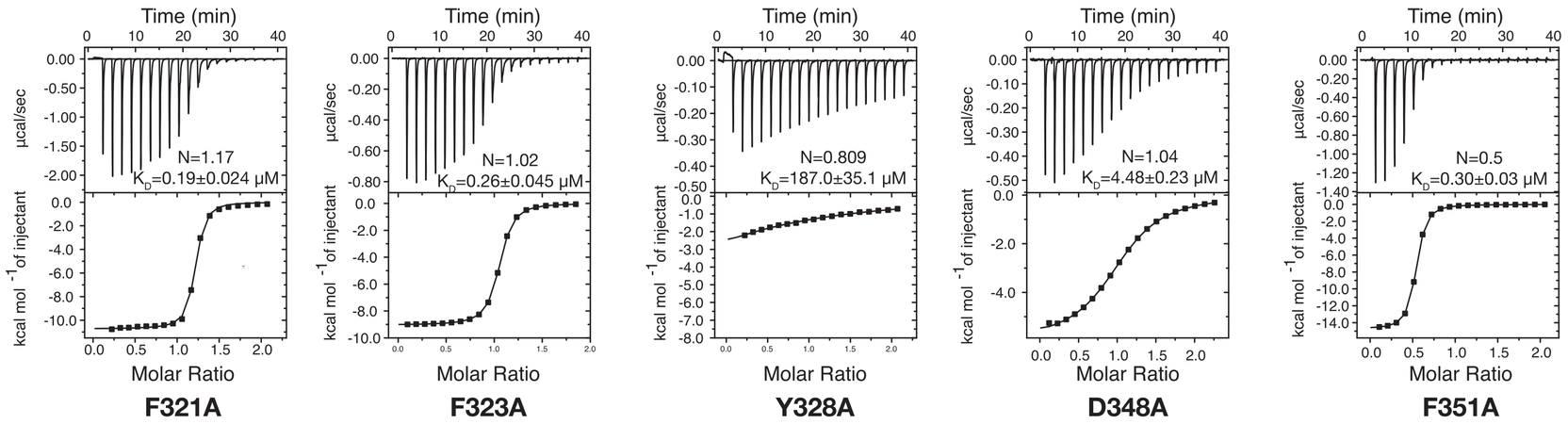

F321A | **F323A** | **Y328A** | **D348A** | **F351A**

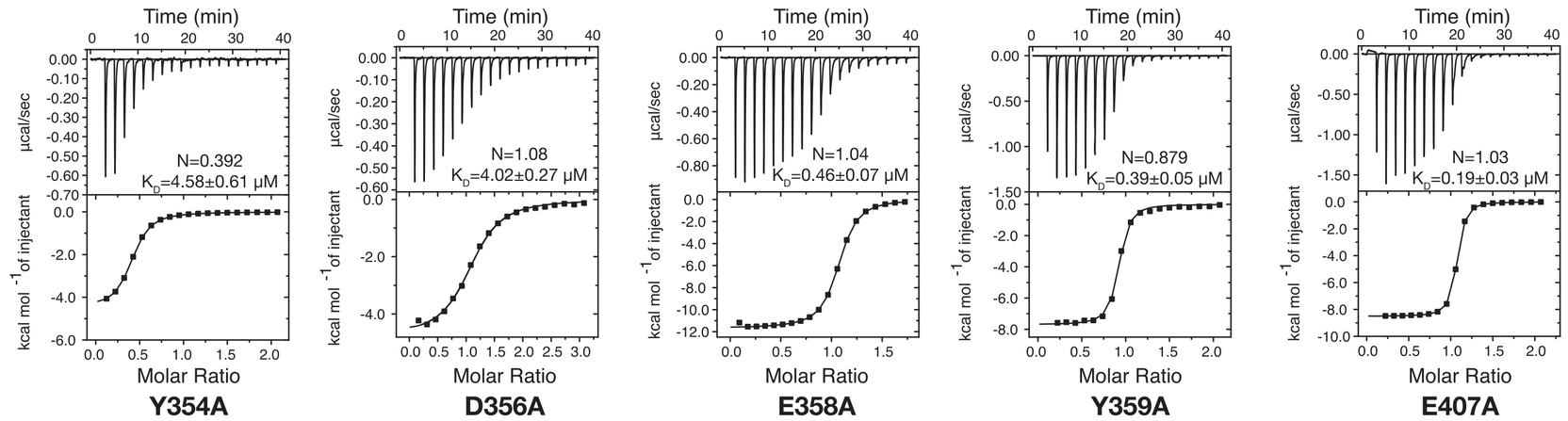

Y354A | **D356A** | **E358A** | **Y359A** | **E407A**

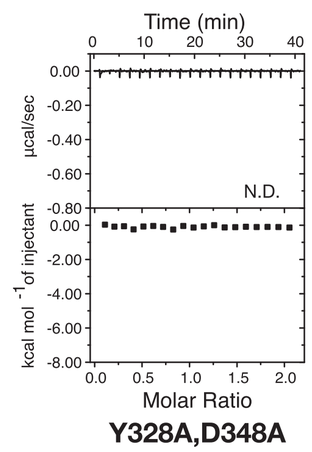

Y328A,D348A

Fig. S11. (Continued)

D

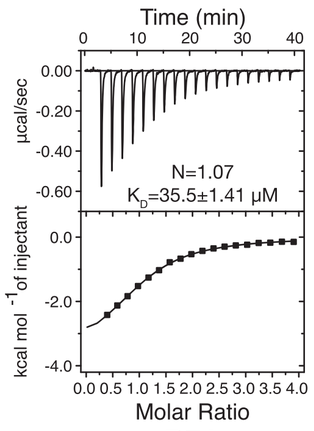

R7A

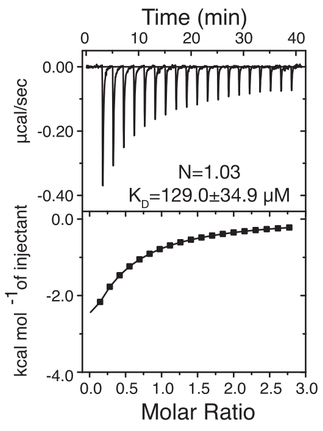

G8V

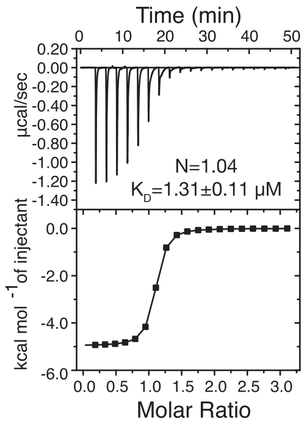

R9A

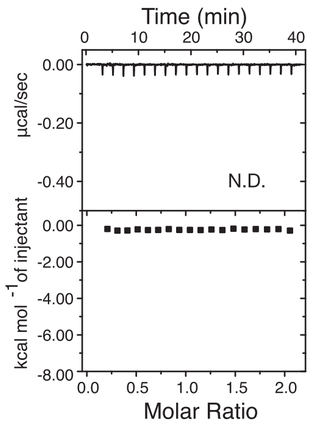

R10A

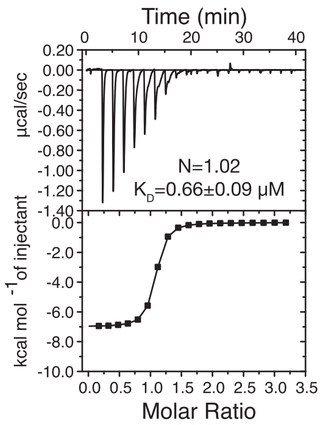

R11A

E

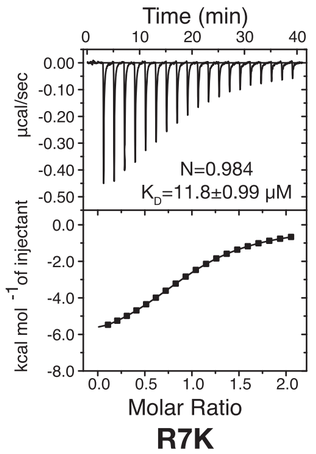

R7K

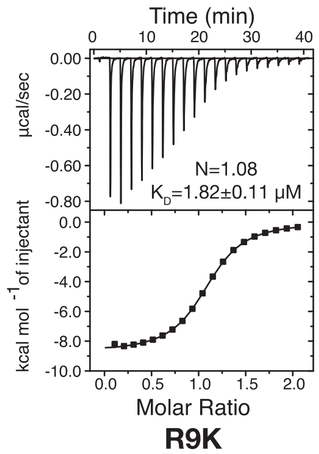

R9K

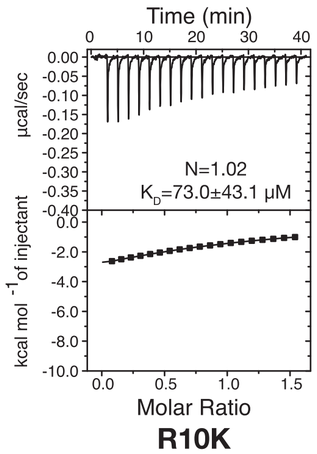

R10K

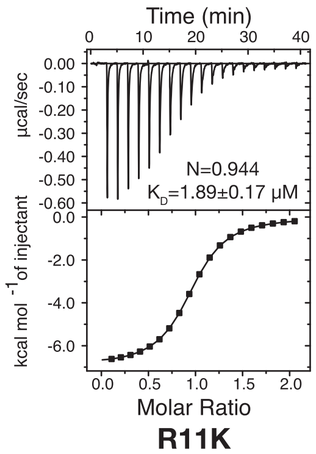

R11K

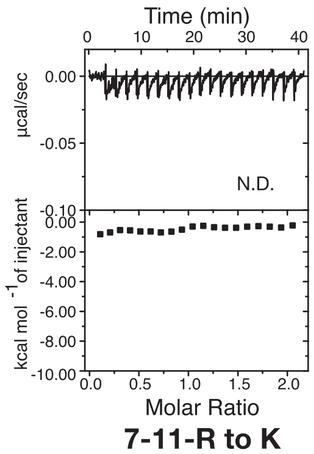

7-11-R to K

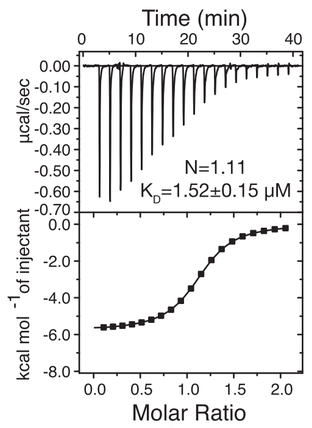

Q5A

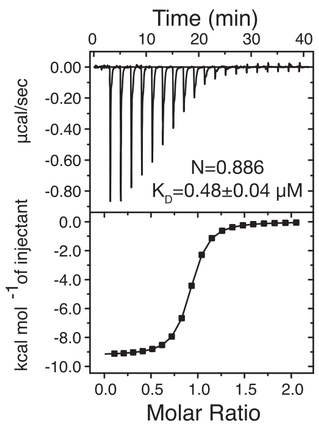

P12A

F

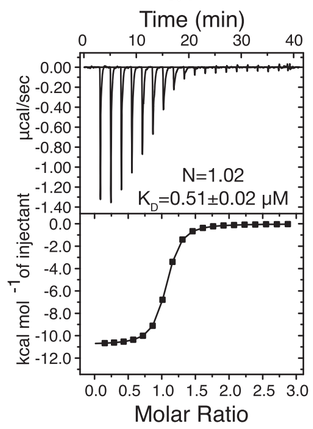

F321A

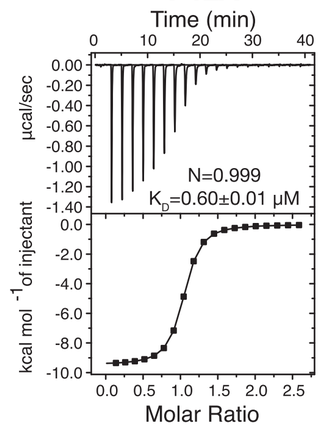

F323A

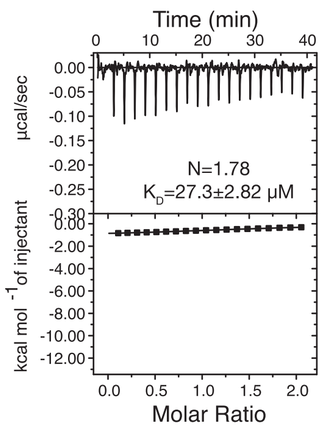

Y328A

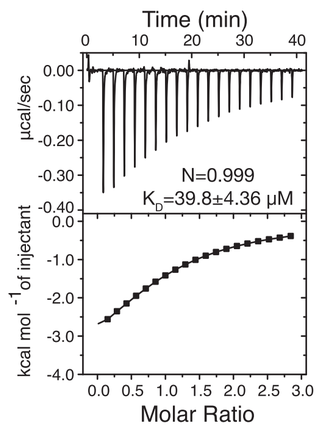

D348A

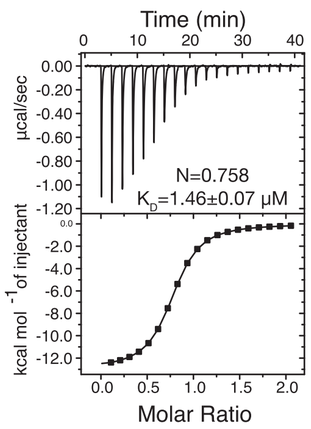

F351A

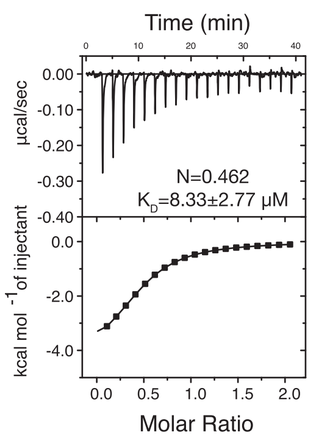

Y354A

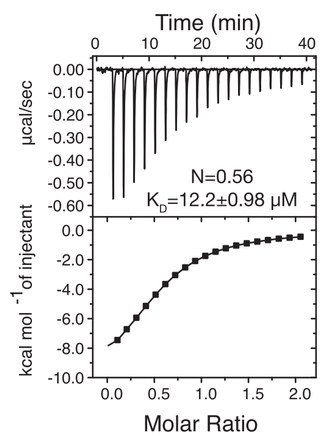

D356A

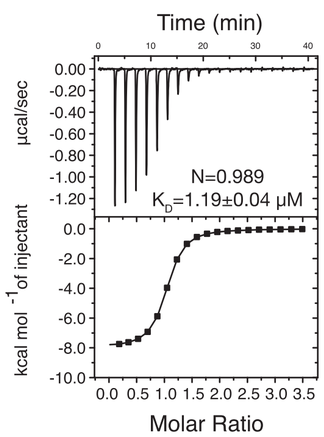

E358A

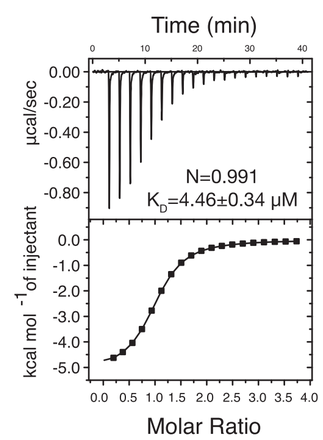

Y359A

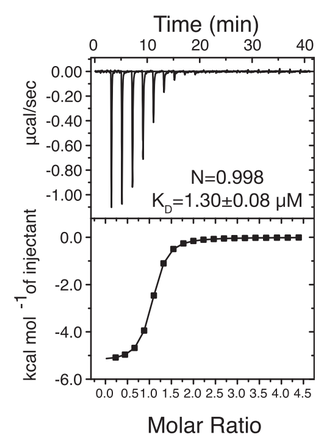

E407A

Fig. S11. (Continued)

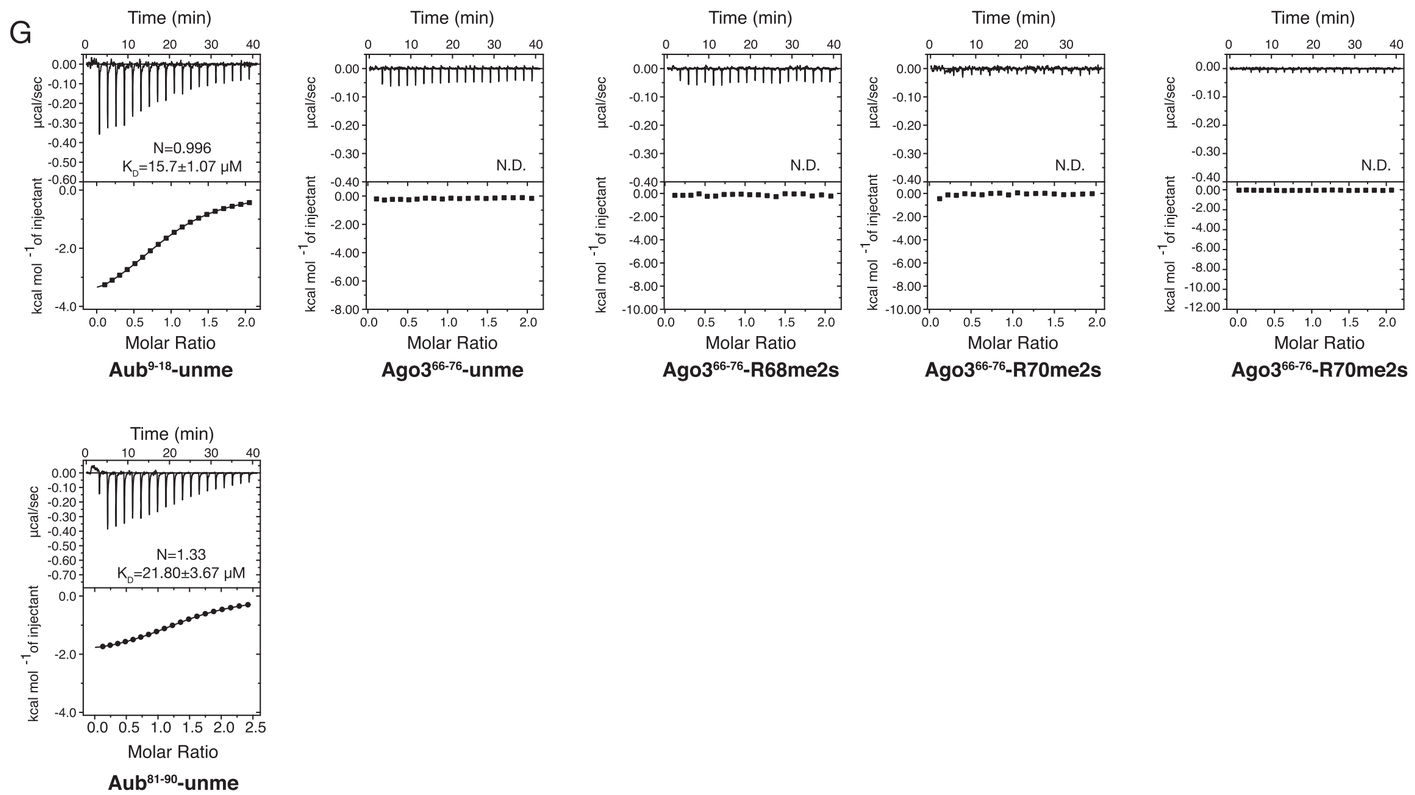

Fig. S11. Raw ITC plots. Shown are raw ITC data related to Fig. 1*D* (*A*), Fig. S1*B* (*B*), Fig. 3*A* (*C*), Fig. 3*B* (*D*), Fig. 3*C* (*E*), Fig. 3*F* (*F*), and Fig. S7*F* (*G*). The ITC data were fit in 1:1 binding mode. K_d values are indicated.

Table S1. Data refinement and refinement statistics

	Papi-apo	Papi-D287A	Papi–Piwi	Papi–Piwi-R10me2s
Data collection				
Space group	$P6_522$	$P4_1$	$P4_1$	$P4_1$
Cell dimensions				
a, *b*, *c*, Å	77.8, 77.8, 144.0	72.2, 72.2, 50.6	72.7, 72.7, 50.4	72.5, 72.5, 50.3
α, β, γ, °	90, 90, 120	90, 90, 90	90, 90, 90	90, 90, 90
Wavelength, Å	0.9778	0.9777	0.9785	0.9785
Resolution,* Å	30–2.0 (2.07–2.0)	30–1.40 (1.45–1.40)	30–1.70 (1.76–1.70)	30–1.55 (1.61–1.55)
R_{merge}*	0.10 (0.33)	0.06 (0.24)	0.08 (0.32)	0.06 (0.43)
$I/\sigma(I)$*	36.2 (4.0)	48.1 (7.2)	36.2 (4.3)	34.1 (2.3)
Completeness,* %	99.9 (99.9)	99.3 (98.3)	99.9 (99.9)	99.9 (99.8)
Redundancy*	23.5 (14.4)	11.8 (10.4)	11.4 (9.3)	10.8 (7.4)
Refinement				
Resolution, Å	27.6–2.0	29.4–1.40	29.5–1.70	29.4–1.55
No. reflections	18,114	51,043	29,124	37,809
R_{work}/R_{free}	0.18/0.21	0.17/0.19	0.20/0.24	0.20/0.23
No. atoms				
Protein	1,631	1,727	1,715	1,678
Peptide	Not applicable	Not applicable	76	94
Water	210	388	310	293
Average B				
Protein	17.8	21.1	27.4	29.3
Peptide	Not applicable	Not applicable	35.2	35.4
Water	21.3	10.4	36.7	38.4
Rmsd				
Bonds length, Å	0.009	0.007	0.007	0.007
Bond angles, °	1.34	1.12	1.06	1.10
Ramachandran plot				
Favored, %	99.5	99.5	99.5	98.6
Allowed, %	0.5	0.5	0.5	1.4
Outlier, %	0.0	0.0	0.0	0.0

*Values in parentheses are for highest-resolution shell.

Table S2. Summary of K_d measurements of TDRD proteins and ligands

Protein	Peptide	K_d, μM	ΔH, cal·mol^{-1}	ΔS, cal·mol^{-1}·degree^{-1}	Figure
Papi-eTud					
Wild type	Piwi-R7me2s	24.0 ± 2.93	−3,673 ± 205	9.78	1*D*
Wild type	Piwi-R9me2s	1.77 ± 0.17	−6,633 ± 86.12	4.10	1*D*
Wild type	Piwi-R10me2s	0.057 ± 0.015	−9,727 ± 103.7	−1.78	1*D*, 3*A*, 3*B*, S2*B*, S9*F*
Wild type	Piwi-R11me2s	0.82 ± 0.17	−7,356 ± 88.47	3.51	1*D*
F321A	Piwi-R10me2s	0.19 ± 0.024	−1.072E4 ± 54.7	−6.36	3*A*
F323A	Piwi-R10me2s	0.26 ± 0.045	9,039 ± 111.6	−0.347	3*A*
Y328A	Piwi-R10me2s	187.0 ± 35.1	−8,182 ± 2,458	−10.9	3*A*
D348A	Piwi-R10me2s	4.48 ± 0.23	−5,953 ± 67.37	4.10	3*A*
F351A	Piwi-R10me2s	0.30 ± 0.03	−1.475E4 ± 115.1	−20.4	3*A*
Y354A	Piwi-R10me2s	4.58 ± 0.61	−4,50 3 ± 194.4	10.1	3*A*
D356A	Piwi-R10me2s	4.02 ± 0.27	−4,757 ± 65.64	8.68	3*A*
E358A	Piwi-R10me2s	0.46 ± 0.07	−1.16E4 ± 157.7	−10.4	3*A*
Y358A	Piwi-R10me2s	0.39 ± 0.05	−7,702 ± 63.37	3.10	3*A*
E407A	Piwi-R10me2s	0.19 ± 0.03	−8,510 ± 66.83	1.74	3*A*
Y328A/D348A	Piwi-R10me2s	N.D.	N.D.	N.D.	3*A*
Wild type	Piwi-R10me2s-R7A	35.5 ± 1.41	−3,325 ± 71.24	10.1	3*B*
Wild type	Piwi-R10me2s-G8V	129.0 ± 34.9	−2,561 ± 1,809	6.99	3*B*
Wild type	Piwi-R10me2s-R9A	1.31 ± 0.11	−4,967 ± 30.82	11.6	3*B*
Wild type	Piwi-R10A	N.D.	N.D.	N.D.	3*B*
Wild type	Piwi-R10me2s-R11A	0.66 ± 0.09	−7,008 ± 75.14	4.38	3*B*
Wild type	Piwi-unme	0.57 ± 0.05	−7,039 ± 38.24	4.61	1*D*, 3*C*, 3*F*, S2*B*, S9*F*
Wild type	Piwi-unme-R7K	11.8 ± 0.99	−6,869 ± 191.9	−0.88	3*C*
Wild type	Piwi-unme-R9K	1.82 ± 0.11	−8,729 ± 71.49	−3.52	3*C*
WT	Piwi-unme-R10K	73.0 ± 43.1	−6,586 ± 2,858	−3.54	3*C*
Wild type	Piwi-unme-R11K	1.89 ± 0.17	−6,929 ± 95.31	2.56	3*C*
Wild type	Piwi-unme-4RK	N.D.	N.D.	N.D.	3*C*
Wild type	Piwi-unme-Q5A	1.52 ± 0.15	−5,786 ± 81.96	6.90	3*C*
Wild type	Piwi-unme-P12A	0.48 ± 0.04	−9,241 ± 79.31	−2.62	3*C*
F321A	Piwi-unme	0.51 ± 0.02	−1.080E4 ± 42.91	−8.05	3*F*
F323A	Piwi-unme	0.60 ± 0.01	−9,487 ± 27.96	−3.88	3*F*
Y328A	Piwi-unme	27.3 ± 2.82	−1,109 ± 342.4	17.1	3*F*
D348A	Piwi-unme	39.8 ± 4.36	−4,822 ± 360	3.69	3*F*
F351A	Piwi-unme	1.46 ± 0.07	−1.296E4 ± 110.4	−17.5	3*F*
Y354A	Piwi-unme	8.33 ± 2.77	−1.130E4 ± 612.1	−16.0	3*F*
D356A	Piwi-unme	12.2 ± 0.98	−4,493 ± 844.3	7.92	3*F*
E358A	Piwi-unme	1.19 ± 0.04	−7,979 ± 38.61	−0.108	3*F*
E359A	Piwi-unme	4.46 ± 0.34	−5,150 ± 81.8	6.91	3*F*
E407A	Piwi-unme	1.30 ± 0.08	−5,265 ± 50.7	8.98	3*F*
D287A	Piwi-R10me2s	0.054 ± 0.018	−9,287 ± 32.85	−0.05	S2*B*
D287A	Piwi-unme	0.62 ± 0.07	−6,715 ± 48.73	5.41	S2*B*
Wild type	Aub$^{9-18}$-unme	15.7 ± 1.07	−4,156 ± 377.5	7.8	S9*F*
Wild type	Aub$^{81-90}$-unme	21.8 ± 3.67	−2,073 ± 58.96	14	S9*F*
Wild type	Ago3$^{66-76}$-unme	N.D.	N.D.	N.D.	S9*F*
Wild type	Ago3$^{66-76}$-R68me2s	N.D.	N.D.	N.D.	S9*F*
Wild type	Ago3$^{66-76}$-R70me2s	N.D.	N.D.	N.D.	S9*F*
Wild type	Ago3$^{66-76}$-R72me2s	N.D.	N.D.	N.D.	S9*F*
mTDRKH-eTud	Miwi2$^{2-11}$-unme	0.12 ± 0.01	−1.425E4 ± 175.9	−16.6	S10*C*
BmPapi-eTud	Siwi$^{5-17}$-unme	2.17 ± 0.12	−1.386E4 ± 142.1	−21.4	S10*C*
BmPapi-eTud	Siwi$^{5-17}$-6RK	N.D.	N.D.	N.D.	S10*C*

N.D., not detected.